http://journal.uir.ac.id/index.php/JGEET

E-ISSN : 2541-5794
P-ISSN : 2503-216X

Journal of Geoscience,
Engineering, Environment, and Technology
Vol 9 No 1 2024

RESEARCH ARTICLE

Petrochemistry of Ultramafic Rock in Baula - Pomalaa Ophiolite Complex, Southeast Sulawesi, Indonesia

Rio Irhan Mais Cendra Jaya[1], Laode Ihksan Juarsan[2], Masri[1,*], Al Rubaiyn[2], Syahrul[3], Neni[1], Suci Ramadani[1], Hasria[1]

[1] *Geological Engineering Department, Halu Oleo University, Kendari, Indonesia*
[2] *Geophysical Engineering Deparmetn, Halu Oleo University, Kendari, Indonesia*
[2] *Mining Engineering Department, Universitas Sembilanbelas November, Kolaka, Indonesia*

* Corresponding author: masri@uho.ac.id
Tel.:+6282-296-451-988
Received: Oct 4, 2023; Accepted: Mar 7, 2024.
DOI: 10.25299/jgeet.2024.9.1.14491

Abstract

Baula and Pomalaa Ophiolitic Complexes are part of East Sulawesi Ophiolite (ESO). The ultramafic rocks in the Baula and Pomalaa Ophiolite Complex mainly is peridotite and consist of harzburgite, lherzolite and olivine websterite, mostly serpentinized. Chemical and petrological research has focused on minerals, such as olivine, pyroxene, and spinel. This study examines the tectonic setting and temperature of ultramafic rock formation. Twelve ultramafic rock samples were examined using geothermometers made of pyroxene, petrographic examination, and coexisting olivine and spinel analyses. SEM and petrographic analysis of pyroxene lamellae and mylonite-ultramylonite structures allowed for the measurement of the geothermometer of ultramafic rocks. Using SEM-EDS, the coexistence of olivine and spinel was analyzed to determine the type of ultramafic tectonic setting. In the coexistence of olivine and spinel, olivine and spinel oxide compounds as tectonic setting markers in the form of Fo and Cr# values. Ultramafic rocks have different temperature levels, based on pyroxene thermometer, and the first one starts at a high temperature of 1000-1200ºC. It is characterized by thin, elongated augite lamellae. Instead, large lamellae characterize augite at medium temperatures (800–1000ºC). Irregular, anhedral, and broader forms of enstatite lamellae are typical of low temperatures (500–800ºC). Different generations of exsolution lamellae indicate that magma cooling was gradual. The distribution of #Fo ranged from 0.87 to 0.92, and Cr# values ranged from 0.13-0.19. According to coexisting olivine and spinel analysis. On the Olivine-Spinel Mantle Array (OSMA), the Fo and Cr# plot indicates that the peridotites tectonic setting was from the ocean floor and the magmatism was from MORB (Mid Oceanic Ridge Basalt). The Al_2O_3 vs. TiO_2 pattern in spinel lherzolite also similar with Ampana and Kabaena peridotites magmatism.

Keywords: pyroxene lamella, geothermometer, olivin-spinel coexisting, MORB peridotite, Kolaka

1. Introduction

In Indonesia, Ophiolite complexes are located in Meratus Mountains, eastern and southeastern Sulawesi, Halmahera, and Papua. Some ophiolite complexes are associated with melange, such as in Ciletuh (West Java), Karangsambung (Central Java), and Bantimala (Sulawesi) (Surono and Hartono, 2013). The ophiolite complex on Sulawesi Island is known as the East Sulawesi Ophiolite Belt (ESOB) or the East Sulawesi Ophiolite Belt (LOST). The LOST extends for 500 km along the eastern arm to the southeastern arm (Parkinson, 1998). The LOST can be traced from the East Arm of Sulawesi, starting from Poh, Bunta, to Ampana and Morowali. In the central part of Sulawesi, LOST is distributed in Kolonodale, Bungku, and Kendari. The west coast of the Southeast Arm of Sulawesi, such as Lasusua, Kolaka, and Kabaena (Kadarusman et al., 2004, Hamilton, 1979).

The ophiolites of eastern Sulawesi are Late Cretaceous-Eocene in age and were displaced during the Oligocene-Miocene period by the Sula Spurs collision (Parkinson, 1998). The ophiolite was displaced along a back-arc basin shear fault (Monnier et al., 1995) with an obduction mechanism (Husein et al., 2014). The ophiolite sequence consists of peridotite cumulates, microgabbro, sheeted dolerite, and MORB basaltic (Kadarusman et al., 2004). Peridotites are dunite, harzburgite, lherzolite and pyroxenite, while microgabbro and basalt are only found locally in a few places (Surono, 2013). REE element studies on peridotite clinopyroxene indicate a mid-ocean ridge (MOR) origin rather than a suprasubduction zone. (Kadarusman et al., 2004).

The displacement of ultramafic rocks is important for the study of petrology and petrogenesis because mineralogical parameters related to changes in temperature and pressure during the rock formation process (geothermometer) and displacement can tell us about the early genesis of peridotite rock formation and its tectonic evolution (Lindsley and Andersen, 2012). The formation temperature of ultramafic rocks can be identified based on pyroxene minerals that exhibit lamellar exsolution textures between clinopyroxene and orthopyroxene (Yellappa et al., 2021, Koizumi et al., 2014, Lindsley, 1983). The exsolution process usually occurs due to lamellae growth in the crystal of origin during the cooling process. The determination of the tectonic environment of ultramafic rocks is based on the presence of coexisting olivine and spinel minerals (Olfindo et al., 2020, Payot et al., 2018, Arai, 1994).

The research location for the study of petrology and mineral chemistry of ultramafic rocks is at Pomalaa and Baula, Kolaka Regency, Southeast Sulawesi Province. In this area, there are widely exposed ultramafic rocks, which have generally been serpentinized (Jaya, 2017, Simandjuntak et al., 1993). The research proposal is predicated on the dearth of pertinent studies about the petrology and mineral chemistry of ultramafic rocks in this region.

In this study, the formation temperature of ultramafic rocks was analyzed by making petrographic observations and

analyzing pyroxene lamellae (geothermometer) using SEM. This data was then combined with the results of chemical analysis of coexisting olivine-spinel to obtain an overview of the tectonic environment of the study area.

2. Methodology

A descriptive approach to field geology methods, supported by laboratory analysis, is used to conduct this research. The percentage of mineral composition in petrographic observations has been the subject of quantitative research. Megascopically and microscopically detailed descriptions of ultramafic rock samples serve as primary data.

Fresh ultramafic rocks in the study area are the focus of research. The object was then concentrated on the orthopyroxene-clinopyroxene minerals, which form lamellar exsolution textures, as well as the coexisting olivine and spinel minerals. Thin sections of ultramafic rocks show the presence of these textures. The microscopic description of ultramafic rocks is based on the work of Streckeisen (1976).

The petrographic analysis uses Nikon Eclipse E-100 polarizing microscope at the Geological Engineering Laboratory of Halu Oleo University, with thin sections prepared at the Petrology Laboratory of Hasanuddin University, Makassar. Observed optical properties include crystal shape and size, cleavage, relief, index of refraction, absorbs and pleochroic color, interference color, optical orientation, twinning, and extinguishing angle. This description seeks to identify various characteristics of the olivine and pyroxene minerals present in the thin section, such as specific mineral types, distinctive textures, and other distinguishing characteristics.

If two pyroxene minerals are observed coexisting and forming lamellar exsolution, the formation temperature (geothermometer) of ultramafic rocks can be determined. The two pyroxene minerals analyzed contain clinopyroxene lamellae within an orthopyroxene mineral host. SEM and polarizing microscopy were used to examine these two pyroxene minerals. The formation temperature of ultramafic rocks requires a descriptive analysis based on the texture and chemical composition of lamellar pyroxene.

A Phenom ProX SEM equipped with an EDS detector was used to determine the mineral's chemical composition. Utilizing the EDS detector, chemical data on minerals was gathered. With 15 kV of accelerating voltage and 30 mA of probe current, mineral chemistry tests were conducted in a high vacuum environment. There are sixteen firing points (beams), each of which is composed of a lamellar-forming orthopyroxene-clinopyroxene mineral and a coexisting olivine-spinel mineral. The elements measured include Oxygen (O), Magnesium (Mg), Silicon (Si), Iron (Fe), Nickel (Ni), Calcium (Ca), Aluminum (Al), Manganese (Mn), Chromium (Cr), Titanium (Ti), Sodium (Na), Potassium (K), Zinc (Zn), and Vanadium (V) (V). The chemical data is presented as oxide compounds with weight percent (wt percent) units, including SiO_2, MgO, FeO, NiO, CaO, MnO, Al_2O_3, Cr_2O_3, TiO_2, K_2O, Na_2O, ZnO, and V_2O_3. The weight percent (wt percent) data were analyzed and processed in order to determine the mole percent (percent mol) of Mg (percent En), Fe (percent Fs), Ca (percent Wo), Cr#, Mg#, and others.

Together-growing olivine and spinel minerals (coexisting) were used to determine the tectonic environment of ultramafic rocks in the study area. Using SEM-EDS analysis, chemical data were obtained based on the work of Arai (1994).

3. Geology

3.1 Geomorphology

The geomorphology of the Baula-Pomalaa area, Kolaka Regency, consists of hills, valleys, and lowlands at 0-800 meters above sea level elevation. Based on van Zuidam (1986) classification, the study area is divided into three geomorphological units, i.e. structural morphology (55%), which is spread in the central and northeast-southeast part of the study area, denudational morphology (40%) which is distributed in the west-southwest part of the study area, and fluvial system (5%) which is spread in the northwest part of the study area. River systems consist of rectangular and dendritic patterns. Rectangular type is found almost throughout the study area, with igneous and metamorphic rocks. The dendritic flow pattern is located southwest to northwest of the study area, consisting of conglomerate rocks and alluvial deposits.

3.2 Stratigraphy

The stratigraphy of the Baula-Pomalaa area comprises ultramafic rocks, metamorphic rocks, monomic conglomerates, polymictic conglomerates, and alluvial deposits. Ultramafic rocks consist of peridotite. The primary minerals of ultramafic rocks are olivine, pyroxene, and spinel. The secondary minerals consist of serpentine, chlorite, and talc. Both ultramafic and metamorphic rocks are separated by structural contact of fault. In general, ultramafic rocks have undergone partial or complete serpentinization and have been weathered into laterite deposits. Ultramafic rocks occupy ~40% of the study area (**Fig 1**).

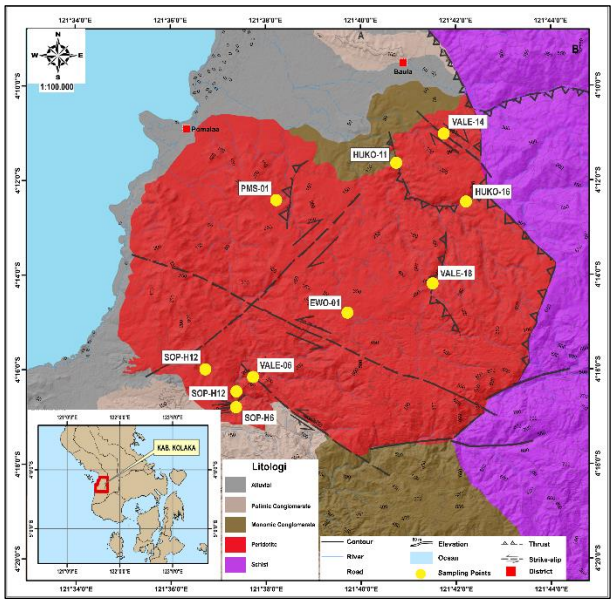

Fig 1. Geologic map and distribution of ultramafic rock sample in the study area

Metamorphic rocks in the study area consist of schist and alteration rock serpentinite. Serpentinites are composed of serpentine minerals such as lizardite and chrysotile. Muscovite-quartz schists dominate the schists in the study area and belong to the greenschist facies. The schists are scattered in the eastern part of the study area.

Conglomerates in study area are consist of two type, monomic and polymictic conglomerates. Monomic conglomerates are found in isolated intra-mountain depressions and rivers with >10m fault scarp. Isolated intra-mountain basin formed by tectonic uplift of ophiolite onto metamorphic basement. During that time, conglomerate was formed by ultramafic fragments which deposited in the basin (Surono, 2013). The conglomerates grain fragments are dominated by ultramafic rocks and serpentinite (>90%). The grain size is sand-boulder (>30 cm), dark brown-brown in color, non-

carbonate cement, and poor sorted and generally distributed in the southern part and slightly in the north of the study area.

The polymictic conglomerate is found in low-elevation areas in the south-southwest and slightly north of the study area. This area is located outside of isolated basin. Its grain consists of ultramafic, schist, serpentinite, and limestone lithics with boulder-sand size (<30 cm), light grey-brown, non-carbonate cement, and poorly sorted. In some locations, these rocks have not consolidated well.

Alluvial deposits are found in the north and along the coastline of the study area. This area is generally for residential use. The alluvium unit consists of brownish-grey to reddish clay-boulder loose material.

3.3 Geological Structure

Geological structures that develop in the study area are strike-slip and thrust faults (**Fig 1**). The regional tectonics influences the formation of the geological structure of the study area in Sulawesi, which has the direction of the regional structure northwest-southeast. Thrust faults are generally northwest-south-southeast and northeast-southwest, and strike-slip faults are northwest-southeast and northeast-southwest. The formation of structures in the study area is closely related to the collision direction between Southeast Sulawesi and the Buton Microcontinent Fragment which occurred during the Early Miocene and continued until the Late Miocene.

4. Results

4.1 Petrography of Ultramafic Rocks

The ultramafic rocks in the Baula Pomalaa Ophiolite Complex mainly is peridotite and consist of harzburgite, lherzolite and olivine websterite, mostly serpentinized. Ultramafic rocks are structurally adjacent to metamorphic rocks; in some locations, the ultramafic rocks are fully serpentinized. Conglomerates are divided into polymictic and monomic conglomerates, with a predominance of ultramafic grains or fragments. Monomic conglomerates are commonly found in isolated intra-mountain depressions and rivers with >10m inclines. The grain fragments are dominated by ultramafic and serpentinite rocks (>90%). Polymictic conglomerates are found in low elevation areas, outside of isolated basin, with ultramafic rocks, schist, serpentinite and limestone grains.

Based on petrographic analysis of 12 thin sections, ultramafic rocks can be grouped into three types. based on Streckeisen (1976), harzburgite, lherzolite, and olivine websterite. Harzburgite was identified in samples SOP-H12, EWO-01, and PMS-01, lerzolite was identified in samples BDM-01, HUKO-H11, HUKO-H16, SOP-H6, VALE-H14, VALE-H18, and VALE-H6, while olivine websterite was identified in samples PSRD-01 and VALE-02. Generally, olivine is present both as relicts and in subhedral crystal, and mostly serpentinized. (**Table 1**).

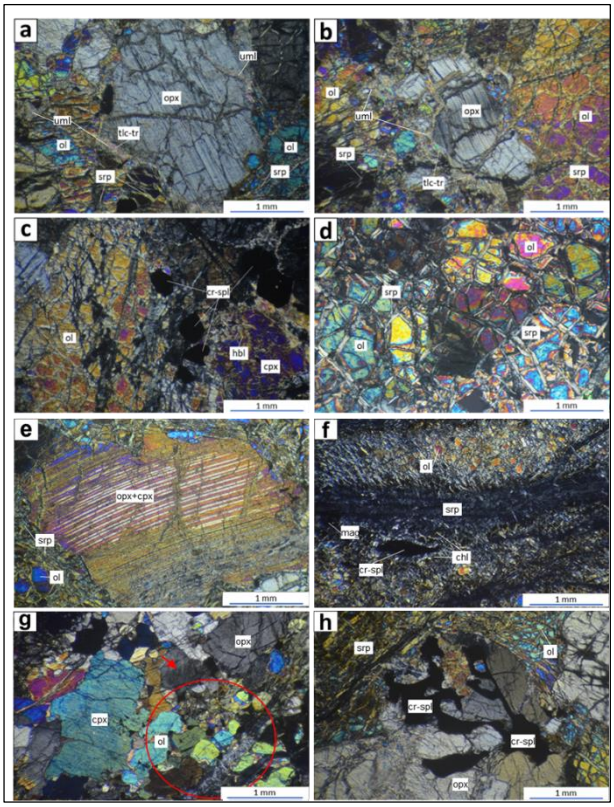

Fig 2. (a) Microphotography of harzburgite (PMS 01) under cross-polarization, showing serpentinized olivine (ol) and orthopyroxene (opx). Ultramilonite (uml) olivine is present on the rim of orthopyroxene. Alterations of orthopyroxene, tremolite (tr) and talc (tlc) are also present in the rim of orthopyroxene (opx). (b) Orthopyroxene (opx), enstatite, on lherzolite (HUKO H16) as host mineral shows a *kinkband* texture (due to brittle deformation) with clinopyroxene (cpx), augite, as lamellar exsolution. Tremolite (tr) and talc (tlc) present as rim alteration of orthopyroxene (opx). Olivine (ol) is partially altered to serpentine (srp), and in contact with orthopyroxene (opx), olivine ultramilonite (uml) is formed due to intensive deformation processes. (c) Lerzolite (HUKO H16) shows some chromite-spinel (cr-spl) crystals coexisting with serpentinized olivine (ol). Clinopyroxene (cpx), augite, appears to be replaced by hornblende (hbl). (d) Harzburgite (SOP H12), with olivine (ol) partially altered to serpentine (srp), showing serpentine (srp) mesh texture. (e) Lamellar exsolution of orthopyroxene (opx) and clinopyroxene (cpx) in Lerzolite (HUKO H16). (f) Lerzolite (VALE 14) showing a chromite spinel-bearing (cr-spl) serpentinized lerzolite. Serpentine (srp) replaces olivine (ol) and exhibits a mesh texture. Chlorite (chl) is present as an alteration mineral. Magnetite (mag) is abundantly distributed and associated with serpentine veins. This magnetite distribution indicates a high degree of serpentinization (Ray et al., 2010) (g) Cumulate orthopyroxene (opx), clinopyroxene (cpx) and olivine (ol) in olivine websterite VALE 02, orthopyroxene (opx) is seen as protomillonite (red arrow) with wavy blackout features, and visible milonite structure in red circle. (h) Irregular chromite spinel (cr-spl) coexisting with serpentinized olivine (ol) and enstatite-type orthopyroxene (opx) in sample VALE 02.

Table 1. Representation of primary and secondary minerals from 12 thin sections of ultramafic rocks. Mineral symbols based on Whitney and Evans (2009). Superscript 'R' = relic, 'X' = lamellar exsolution

Sample	Main Minerals	Secondary Minerals	Lithology
BDM-01	Ol^R + Opx + Cpx	Srp + Tlc	Lerzolit
EWO-01	Ol^R + Opx + Cpx + Cr-Spl	Srp + Tlc + Mag	Harzburgit
PSRD-01	Ol^R + Opx + Cpx	Srp + Chl + Mag	Olivin Websterit
HUKO-H16	Ol + Opx + Cpx^X + Cr-Spl	Srp + Chl + Tr	Lerzolit
HUKO-H11	Ol^R + Opx + Cpx	Srp + Tlc + Chl	Lerzolit
PMS-01	Ol + Opx + Cpx^X + Cr-Spl	Srp + Chl + Tr	Harzburgit
SOP-H12	Ol + Opx + Cpx+ Cr-Spl	Srp + Chl	Harzburgit
SOP-H6	Ol^R + Opx + Cpx + Cr-Spl	Srp + Tlc + Mag	Lerzolit
VALE-H14	Ol + Opx + Cpx + Cr-Spl	Srp + Chl + Mag	Lerzolit
VALE-H18	Ol^R + Opx + Cpx^X + Cr-Spl	Srp + Tlc + Chl	Lerzolit
VALE-H6	Ol^R + Opx + Cpx + Cr-Spl	Srp + Tlc + Mag	Lerzolit
VALE-02	Ol + Opx + Cpx + Cr-Spl	Srp + Chl + Tlc	Olivin Websterit

Harzburgite (EWO 01, PMS 01, and SOP H12) is generally composed of olivine (45-70%), orthopyroxene (20-40%), chromite-spinel (<5%), and clinopyroxene (5-15%). Harzburgite has generally undergone partial serpentinization (**Fig a** and **2d**). Orthopyroxene is present as 1-5 mm subhedral–anhedral crystals, mostly are enstatite. The center of enstatite crystals is generally serpentinized, while the rim, usually in contact with olivine, is altered to tremolite and talc (**Fig a**). Clinopyroxene is present as lamellar exsolution alongside orthopyroxene, mostly are augite and diopside. The chromite-spinel present generally coexisting with olivine. Olivine typically has euhedral-anhedral crystals measuring 0.2-3 mm, altered to serpentine, forming vein and mesh textures (**Fig d**). At some contacts between olivine and orthopyroxene, olivine is also present as milonite and ultramilonite (**Fig a**). Ultraminolites indicate an intensive deformation process in the shear zone (Matysiak and Trepmann, 2015). The magnetite present is a by-product of the serpentinization process (Maulana et al., 2015).

Lherzolites (HUKO H16 and VALE H14) are generally composed of olivine (40-50%), orthopyroxene (20-30%), clinopyroxene (25-30%), and chromite-spinel (<5%). The serpentinization process of lherzolite in the study area is more intensive than that of harzburgite (**Fig f**). Orthopyroxene is present as subhedral-anhedral crystals of 0.5-5 mm in size, mostly are enstatite. Tremolite-talc and olivine ultramilonite are present at the rim of enstatite in contact with olivine (**Fig b**). One of the enstatite crystals was also found to have a kinkband texture, and some had undulate extinction (**Fig b**). These textures are characteristic of rigid/brittle deformation (Kadarusman et al., 2004). Augite is present as subhedral-anhedral crystals of 1-5 mm size and as lamellar exsolution within the host mineral enstatite (**Fig b** and **2e**). Hornblende was found to start partially replacing augite (**Fig c**). Chromite-spinel is found generally coexisting with olivine (**Fig c**). Olivine typically has euhedral-anhedral crystals measuring 0.1-3 mm, altered to serpentine and chlorite, forming vein and mesh textures (**Fig c** and **2f**).

5. Mineral Chemistry of Ultramafic Rocks

5.1 Olivin

Olivine mineral chemistry data (4 oxygen) were normalised, assuming all Fe is Fe^{2+}. All olivine minerals analyzed were forsterite $([Fe,Mg]_2SiO)_4$ with Fo contents varying from 0.87 - 0.92 (**Table 2**).

5.2 Orthopyroxene

The chemical data of orthopyroxene minerals in ultramafic rocks of the Baula and Pomalaa Regional Ofiolite Complex can be seen in **Table 3**. The orthopyroxene mineral chemistry data is normalized (6 oxygen) with a total cation of 4 apfu. Orthopyroxene is present in all ultramafic rock incisions and is of the Mg-rich enstatite type with compositions $En_{87,1\text{-}88,5}$, $Fs_{9,1\text{-}10,8}$, $Wo_{2,05\text{-}2,9}$. X_{Mg} range ~0.92.

5.3 Clinopyroxene

The chemical data of clinopyroxene minerals of ultramafic rocks of the Ophiolite Complex of Baula and Pomalaa Regions can be seen in **Table 3**. The mineral chemistry data of orthopyroxene is normalized (6 oxygen) with a total cation of 4 apfu. Mg-rich clinopyroxene is present in some ultramafic rock incisions and is predominantly of the augite and diopside types. Augite has a composition of $En_{50,8\text{-}55,2}$, $Fs_{4,6\text{-}5}$, $Wo_{38,6\text{-}44,1}$ with X_{Mg} ~0.92. Diopsids have compositions $En_{47,08}$, $Fs_{4,66}$, $Wo_{48,26}$ with X_{Mg} ~0.91.

5.4 Chromite-spinel

The chemical data of spinel mineral of ultramafic rock of the Ophiolite Complex of Baula and Pomalaa Area can be seen in **Table 2**. The spinel mineral chemistry data (4 oxygen) is normalized with a total cation of 3 apfu. All spinel minerals analyzed at the study sites are chromite-spinel type ($[Mg,Fe][Cr,Al]_2O_4$) with Cr# <0.2.

Table 2. Chemical data of coexisting olivine (ol) and spinel (spl) minerals (HUKO H16)

HUKO H16	Ol	Spl	Ol	Spl	Ol	Spl	Ol	Spl
SiO_2	40,00	0,30	36,32	0,38	38,57	0,47	44,58	0,81
TiO_2	0,00	0,00	0,00	0,03	0,00	0,03	0,00	0,00
Al_2O_3	0,00	53,64	0,22	49,72	0,43	53,11	0,15	49,16
Cr_2O_3	1,22	11,85	0,02	17,86	0,08	15,25	0,02	15,69
FeO	8,45	12,89	12,86	13,80	10,70	12,37	7,12	11,37
MnO	0,07	0,27	0,07	0,15	0,02	0,11	0,10	0,34
MgO	51,30	20,31	50,34	17,09	48,74	17,97	46,85	21,68
NiO	0,19	0,00	0,31	0,00	0,25	0,00	0,36	0,00
CaO	0,01	0,07	0,28	0,00	0,28	0,00	0,25	0,01
Na_2O	0,00	0,00	0,00	0,00	0,00	0,00	0,00	0,00
K_2O	0,00	0,00	0,00	0,00	0,00	0,00	0,00	0,00
ZnO	0,00	0,22	0,00	0,00	0,00	0,00	0,00	0,26
V_2O_3	0,00	0,02	0,00	0,00	0,00	0,00	0,00	0,00
Total	101,24	99,57	100,42	99,03	99,07	99,31	99,43	99,32
Si	0,96	0,01	0,89	0,01	0,95	0,01	1,10	0,02
Ti	0,00	0,00	0,00	0,00	0,00	0,00	0,00	0,00
Al	0,00	1,66	0,01	1,59	0,01	1,67	0,00	1,53
Cr	0,02	0,25	0,00	0,38	0,00	0,32	0,00	0,33
Fe^{3+}	0,00	0,08	0,00	0,00	0,00	0,00	0,00	0,09
Fe^{2+}	0,17	0,21	0,26	0,31	0,21	0,28	0,15	0,16
Mn	0,00	0,01	0,00	0,00	0,00	0,00	0,00	0,01
Mg	1,84	0,80	1,83	0,69	1,80	0,72	1,73	0,86
Ni	0,00	0,00	0,01	0,00	0,00	0,00	0,01	0,00
Ca	0,00	0,00	0,01	0,00	0,01	0,00	0,01	0,00
Na	0,00	0,00	0,00	0,00	0,00	0,00	0,00	0,00
K	0,00	0,00	0,00	0,00	0,00	0,00	0,00	0,00
Zn	0,00	0,00	0,00	0,00	0,00	0,00	0,00	0,01
V	0,00	0,00	0,00	0,00	0,00	0,00	0,00	0,00
Total	3,00	3,00	3,00	3,00	3,00	3,00	3,00	3,00
Fo	0,91		0,87		0,89		0,92	
Cr/(Cr+Al)		0,13		0,19		0,16		0,18
Cr/(Cr+Al+Fe3+)		0,12		0,19		0,16		0,17
Al/(Cr+Al+Fe3+)		0,84		0,81		0,84		0,78
Fe3+/(Cr+Al+Fe3+)		0,04		0,00		0,00		0,05
Mg/(Mg+Fe3+)		0,91		1,00		1,00		0,90

6. Discussion

6.1 Geothermometer

The geothermometer or formation temperature of ultramafic rocks in this study was determined using two pyroxene thermometers, lamellar exsolution between orthopyroxene and clinopyroxene (Lindsley, 1983). The formation temperature of ultramafic rocks can be obtained through lamellar exsolution of orthopyroxene and clinopyroxene, provided that the content of wolastony + enstatite + ferrophyllite amounts to ≥90%. The diagram used in determining the formation temperature is the enstatite-diopsid-hedenbergite-ferosilite (En-Di-Hd-Fs) quadrilateral diagram with a pressure of 5 kbar (Lindsley and Andersen, 2012). The quadrilateral diagram of En-Di-Hd-Fs at a pressure of 5 kbar is used based on Kadarusman et al. (2004) on the metamorphism process of amphibolite facies in the ophiolite complex in Sulawesi that occurred at a pressure of about 4 kbar.

Based on the %mol En, Fs, Wo data of orthopyroxene and clinopyroxene lamellar exsolution in **Table 3** plotted in the En-Di-Hd-Fs quadrilateral diagram at a pressure of 5 kbar, three temperature groups of pyroxenes crystallization were obtained. These three temperature groups are located on different temperature lines (**Fig**). Low temperature rock formation data has a temperature interval of 500-800ºC. Medium temperature rock formation data which has a temperature interval of 800-1000ºC. High-temperature rock formation data has a temperature interval of 1000-1200ºC.

Table 3. Chemical data of orthopyroxene (opx) and clinopyroxene (cpx) minerals forming lamellar exsolution (PMS 01)

PMS 01	Cpx1	Opx1	Cpx2	Opx2	Cpx3	Opx3	Cpx4	Opx4
Mineral	Augite	Enstatite	Diopsite	Enstatite	Augite	Enstatite	Augite	Enstatite
SiO_2	52,02	55,77	52,94	53,31	52,30	55,64	52,86	54,95
TiO_2	0,70	0,25	0,58	0,26	0,56	0,11	0,65	0,28
Al_2O_3	4,04	3,66	3,02	3,98	3,49	3,43	3,98	4,17
Cr_2O_3	1,16	1,06	0,80	0,59	0,83	0,76	1,27	0,89
FeO	2,93	6,77	2,80	6,79	4,01	6,08	3,16	6,02
MnO	0,05	0,06	0,02	0,11	0,10	0,10	0,05	0,09
MgO	17,39	30,55	15,88	34,25	20,19	32,23	17,89	32,81
NiO	0,00	0,00	0,00	0,00	0,00	0,00	0,00	0,00
CaO	20,95	1,00	22,65	1,51	19,65	1,48	21,64	1,21
Na_2O	0,26	0,00	0,18	0,01	0,00	0,13	0,21	0,01
K_2O	0,02	0,00	0,01	0,02	0,00	0,01	0,02	0,00
ZnO	0,00	0,00	0,00	0,00	0,00	0,00	0,00	0,00
V_2O_3	0,00	0,00	0,00	0,00	0,00	0,00	0,00	0,00
Total	99,52	99,12	98,88	100,83	101,13	99,97	101,73	100,43
Si	1,90	1,97	1,96	1,82	1,87	1,93	1,89	1,89
Ti	0,02	0,01	0,02	0,01	0,02	0,00	0,02	0,01
Al	0,17	0,15	0,13	0,16	0,15	0,14	0,17	0,17
Cr	0,03	0,03	0,02	0,02	0,02	0,02	0,04	0,02
Fe^{3+}	0,00	0,00	0,00	0,17	0,07	0,00	0,00	0,01
Fe^{2+}	0,09	0,20	0,09	0,02	0,05	0,18	0,09	0,17
Mn	0,00	0,00	0,00	0,00	0,00	0,00	0,00	0,00
Mg	0,95	1,61	0,88	1,74	1,07	1,67	0,95	1,68
Ni	0,00	0,00	0,00	0,00	0,00	0,00	0,00	0,00
Ca	0,82	0,04	0,90	0,06	0,75	0,05	0,83	0,04
Na	0,02	0,00	0,01	0,00	0,00	0,01	0,01	0,00
K	0,00	0,00	0,00	0,00	0,00	0,00	0,00	0,00
Zn	0,00	0,00	0,00	0,00	0,00	0,00	0,00	0,00
V	0,00	0,00	0,00	0,00	0,00	0,00	0,00	0,00
Total	4,00	4,00	4,00	4,00	4,00	3,99	4,00	4,00
En	51,01	87,12	47,08	87,50	55,22	87,81	50,80	88,54
Fs	4,82	10,83	4,66	9,73	6,15	9,29	5,03	9,11
Wo	44,17	2,05	48,26	2,77	38,63	2,90	44,16	2,35
Mg#	0,91	0,89	0,91	0,99	0,95	0,90	0,91	0,91

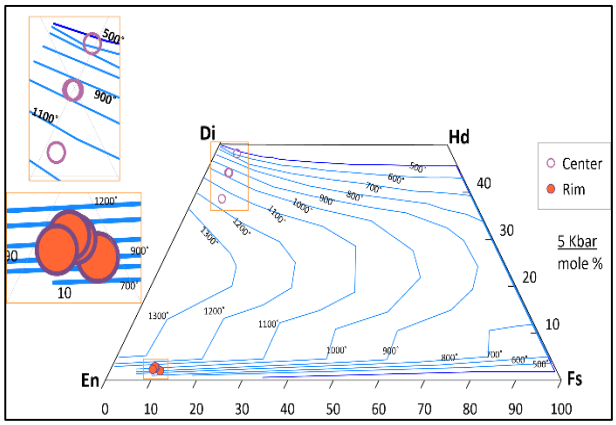

Fig 3. Plot of %mol En, Fs, Wo on En-Di-Hd-Fs quadrilateral diagram at 5 kbar (Lindsley, 1983)

The high-temperature rock formation data, with a temperature interval of pyroxenes crystallization between 1000-1200ºC, is interpreted as the initial crystallization temperature of peridotites. The lamellae texture of augite shown in this high-temperature data has not been disturbed by deformation and is characterized by a thin and straight lamellar. The medium-temperature rock formation data, which has a temperature interval of augite crystallization between 800-1000ºC, is characterized by lamellae texture that has been deformed broader compared to the lamellae texture at high temperatures.

The low-temperature rock formation data, which has a temperature interval of enstatite crystallization between 500-800ºC. The lamellar texture shown in the low-temperature data (**Fig**) is interpreted to have been disturbed by deformation and formed after reheating (Pittarello et al., 2019) due to deformation. Deformation is characterized by the irregular shape of the lamellae and wider dimensions compared to other

lamellae. The reduction of calcium (Ca) changes the shape and dimension of lamellae (Rajesh, 2006).

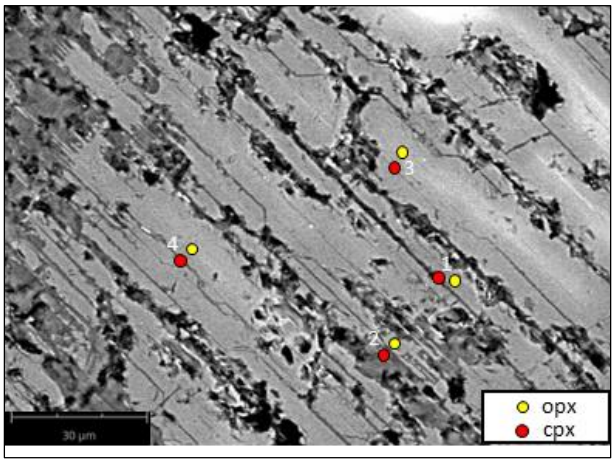

Fig 4. SEM EDS observation of point PMS 01 showing some lamellae textures

The geothermometer estimated pyroxene equilibration temperatures from 1000°C to 1200°C. These temperatures reflect magma-induced pyroxene crystallization. Several lamellar generations of pyroxenes formed at lower temperatures, from 500°C to 1000°C, as the magma cooled. Pyroxenes crystallized over a long cooling period, with different lamellar generations reflecting undercooling and progressive or continuous exsolution (Rajesh, 2006). The thin primary pyroxenes suggest low fractionation at high temperatures, while the broader lines between host and lamellae phases indicate slow cooling that allowed various exsolution textures. Due to slow cooling, different generations of exsolution lamellae developed with different temperatures.

6.2 Petrogenesis of Ultramafic Rocks

According to petrographic analysis, peridotite dominates ultramafic rocks in the study area. The rocks found are peridotite (harzburgite and lherzolite) and pyroxenite (olivine websterite). The absence of garnet in the ultramafic rocks of the Baula and Pomalaa Ophiolite Complexes indicates that the ultramafic rocks have yet to undergo a high degree of metamorphism. The dominant presence of serpentines in all samples indicates intensive metamorphism at low temperatures. Chlorite and serpentine characterize the continuation of retrograde metamorphism at low temperatures (Frost et al., 2013, Arai, 1994). Serpentine+tremolite+magnetite+talc, especially at the pyroxene rim, indicates a reaction between pyroxene minerals and seawater (Zeng et al., 2012). Another source could also be the decomposition of water from previous serpentine formations. These processes likely occurred during the uplift of the ophiolite from the upper mantle to the surface (Arai et al., 2008). The absence of plagioclase in ultramafic rocks indicates that the uplift process of these ultramafic rocks occurred rapidly (Maulana et al., 2015).

The tectonic setting of ultramafic rocks (**Fig**) was determine by putting the Cr# spinel and Fo olivine data from the mineral chemistry of coexisting olivine and spinel (**Table 2**) onto the Olivine Spinel Mantle Array plot (Arai, 1994). Based on these data, it can be seen that the pattern of olivine spinel chemical data in the study area is similar to the four types of theoretical tectonic environments: ocean floor, oceanic hotspot, Japan arcs, and continent. Based on the chemical data pattern of these tectonic environments, in the oceanic hotspot type, the weight percent of TiO_2 is ~1 wt%. The Japan arcs type has several Cr# values >0.5 and Fo <0.87. In the continent type, there are Cr# values >0.5 even up to 0.75; in the ocean floor type, the Fo values range from 0.88-0.92 and Cr# 0.1-0.6. The chemical data distribution of the study area has TiO_2 ~0.03 wt%, Fo 0.87-0.92, Cr# 0.13-0.19, and none of Fo <0.87. Based on the distribution pattern of mineral chemical data, it can be interpreted that the ultramafic rocks in the study area are suitable for the ocean floor type.

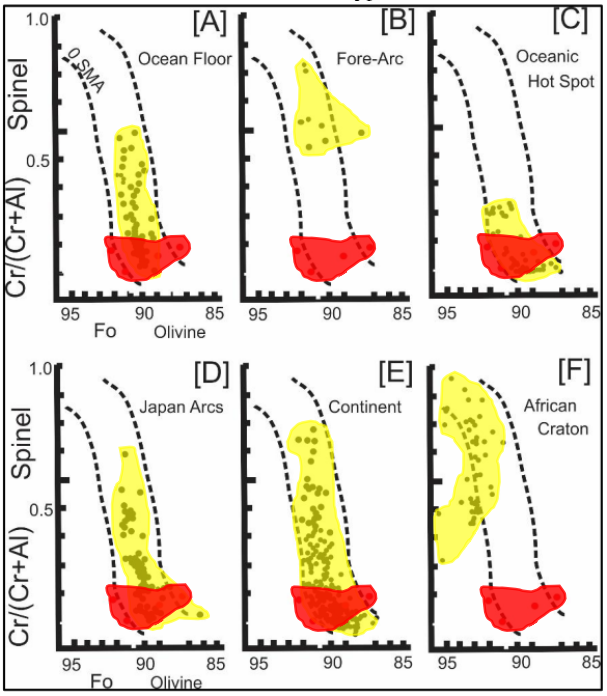

Fig 5. Plot of Cr# spinel vs Fo olivine of ultramafic rocks of Baula-Pomalaa Ofiolite Complex using OSMA diagram. The red shading color is the result of this study and the yellow shading color is the data from Arai (1994).

The Al_2O_3 vs TiO_2 chemical data of the peridotite spinel minerals of the study area were plotted using plot from Kamenetsky et al. (2001) to determine the tectonic setting of the peridotite rocks. The data was then compared with spinel mineral data on Kabaena and Ampana lherzolites (Kadarusman et al., 2004), which have similar distribution patterns (**Error! Not a valid bookmark self-reference.**). Al_2O_3 spinel data distribution in the study area is 46.16-53.64 wt% and TiO_2 ~0.03 wt%. Based on these data, ultramafic rocks are interpreted as the MORB peridotite type.

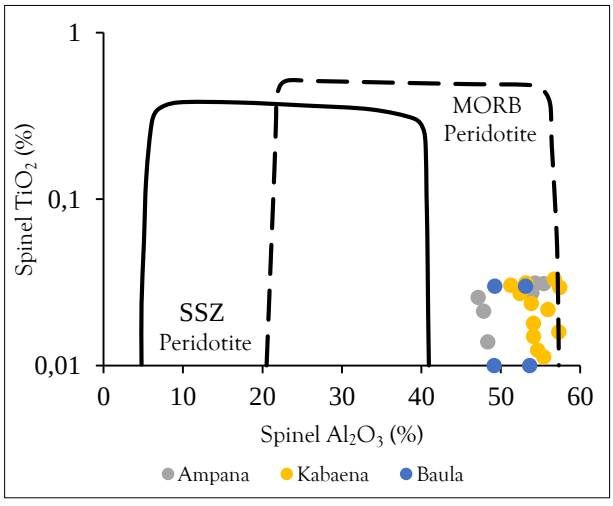

Fig 6. Plot Al_2O_3 vs TiO_2 in spinel peridotite of the study area using graphs from Kamenetsky et al. (2001) compared with data of Al_2O_3 vs TiO_2 in spinel peridotite of Kabaena and Ampana from Kadarusman et al. (2004)

6.3 Tectonic Setting

Based on petrographic analysis, the Baula Pomalaa Ophiolite Complex comprises only ultramafic rocks. The ultramafic rocks encountered are peridotite (harzburgite and lerzolite) and pyroxenite (olivine websterite). In the study area have undergone a very significant tectonic process and produced dismembered ophiolitic sequence (Jaya, 2017, Syahrul, 2017, Maulana et al., 2015).

The speed of the ocean floor spreading results in different characteristics of the ophiolites (Poli and Schmidt, 2002, Pearce et al., 1984). The ophiolite complexes formed through *fast-spreading centers* are characterized by harzburgite, poor clinopyroxene, and dunite (Maulana et al., 2015). The Baula Pomalaa Ophiolite Complex generally consists of harzburgite and lherzolite with abundant clinopyroxene minerals. The dismembered ophiolitic sequence and the abundance of clinopyroxene (augite or diopside) in the ultramafic rocks indicate that the ophiolite sequence formed through slow spreading center mechanism (Gong et al., 2016, Maulana et al., 2015). The pyroxenite (olivine websterite) also indicates that the Baula Pomalaa Ofiolite Complex formed at a slow spreading center.

The formation process of ultramafic rocks can be interpreted based on the formation temperature of lamellar exsolution between orthopyroxene and clinopyroxene minerals. Ultramafic rocks in the study area formed at a temperature of ~1200°C. This temperature is the crystallization temperature of pyroxene minerals. Due to slow cooling, different generations of exsolution lamellae developed with different temperatures.

The chemical data of the ultramafic rocks of the Baula Pomalaa Ofiolite Complex show some similarities with several other ophiolite complexes on Sulawesi Island. The ultramafic rocks of the Southeast Arm of Sulawesi are part of the Cretaceous-aged East Sulawesi Ophiolite (ESO) (Surono, 2013). The data distribution plot of Al_2O_3 vs TiO_2 spinel peridotite of the study area has similarities with the Kabaena and Ampana patterns, which have previously been studied by Kadarusman et al. (2004) and belongs to the East Sulawesi Ofiolite, i.e. the peridotite at the site is sourced from the MORB peridotite. Based on the data plot of Cr# vs Fo and Al_2O_3 vs TiO_2 (Fig 6), it can be concluded that the tectonic setting of ultramafic rocks in the study area is ocean floor with magmatism sourced from MORB (Mid Oceanic Ridge Basalt).

7. Conclusion

Ultramafic rocks in the Baula-Pomalaa Ofiolite Complex are dominated by peridotite (harzburgite, lerzolite) and pyroxenite (olivine websterite). Ultramafic rocks have undergone serpentinization and low-degree metamorphism as evidenced by serpentine, talc, and amphibole minerals (tremolite and hornblende). Based on the geothermometer analysis, the formation temperature of ultramafic rocks is divided into three groups, i.e., high temperature (1000-1200°C) as the initial rock formation temperature characterized by thin elongated lamellae. Intermediate temperatures (800-1000°C) are characterized by a relatively wide type of lamellae in orthopyroxene. Anhedral and wider irregular lamella types characterize low temperatures (500-800°C) which formed after pyroxenes reheating (Pittarello et al., 2019) due to tectonic movement. Coexisting olivine and spinel analysis shows a distribution of Fo values ranging from 0.87-0.92 and Cr# values ranging from 0.13-0.19. The results of the tectonic setting plot on the Olivine-Spinel Mantle Array (OSMA) obtained that the tectonic setting of ultramafic rocks in the study area belongs to the ocean floor with magmatism sourced from MORB (Mid Oceanic Ridge Basalt).

8. Acknowledgements

This research is supported by Halu Oleo University through the Institute for Research and Community Services Funding, through the 2023 Penelitian Dosen pemula (PDP) Research Scheme.

References

Arai, S., Tamura, A., Ishimaru, S., Kadoshima, K., Lee, Y.-I. & Hisada, K.-i. 2008. Petrology of the Yugu peridotites in the Gyeonggi Massif, South Korea: Implications for its origin and hydration process. Island Arc, 17(4). 485-501. https://doi.org/10.1111/j.1440-1738.2008.00633.x

Burnley, P. C., Cline, C. J. & Drue, A. 2013. Kinking in Mg2GeO4 olivine: An EBSD study. American Mineralogist, 98(5-6). 927-931. https://doi.org/10.2138/am.2013.4224

Drue, A. G. 2011. Microstructural characterization of kinked germanate olivine grains. Theses, University of Nevada.

Frost, B. R., Evans, K. A., Swapp, S. M., Beard, J. S. & Mothersole, F. E. 2013. The process of serpentinization in dunite from New Caledonia. Lithos, 178. 24-39. https://doi.org/10.1016/j.lithos.2013.02.002

Gong, X.-H., Shi, R.-D., Griffin, W. L., Huang, Q.-S., Xiong, Q., Chen, S.-S., Zhang, M. & O'Reilly, S. Y. 2016. Recycling of ancient subduction-modified mantle domains in the Purang ophiolite (southwestern Tibet). Lithos, 262. 11-26. https://doi.org/10.1016/j.lithos.2016.06.025

Hamilton, W. B. 1979. Tectonics of the Indonesian Region (Report No. 1078), Professional Paper, U.S. Govt. Print. Off. 345 p. https://doi.org/10.3133/pp1078

Husein, S., Novian, M. I. & Barianto, D. H. 2014. Geological structures and tectonic reconstruction of Luwuk, East Sulawesi Proceedings, Indonesian Petroleum Association: Thirty-Eight Annual Convention & Exhbition, Jakarta, Indonesian Petroleum Association. IPA 14-G-137.

Jaya, R. I. M. C. 2017. Studi petrogenesis dan mineralisasi Kompleks Ofiolit Baula, Kolaka, Sulawesi Tenggara. Thesis, Institut Teknologi Bandung.

Kadarusman, A., Miyashita, S., Maruyama, S., Parkinson, C. D. & Ishikawa, A. 2004. Petrology, geochemistry and paleogeographic reconstruction of the East Sulawesi Ophiolite, Indonesia. Tectonophysics, 392(1-4). 55-83. https://doi.org/10.1016/j.tecto.2004.04.008

Kamenetsky, V. S., Crawford, A. J. & Meffre, S. 2001. Factors Controlling Chemistry of Magmatic Spinel: an Empirical Study of Associated Olivine, Cr-spinel and Melt Inclusions from Primitive Rocks. Journal of Petrology, 42(4). 655-671. https://doi.org/10.1093/petrology/42.4.655

Koizumi, T., Tsunogae, T., Santosh, M., Tsutsumi, Y., Chetty, T. R. K. & Saitoh, Y. 2014. Petrology and zircon U–Pb geochronology of metagabbros from a mafic–ultramafic suite at Aniyapuram: Neoarchean to Early Paleoproterozoic convergent margin magmatism and Middle Neoproterozoic high-grade metamorphism in southern India. Journal of Asian Earth Sciences, 95. 51-64. https://doi.org/10.1016/j.jseaes.2014.04.013

Lindsley, D. H. 1983. Pyroxene thermometry. American Mineralogist, 68(5-6). 477-493.

Lindsley, D. H. & Andersen, D. J. 2012. A two- pyroxene thermometer. Journal of Geophysical Research: Solid Earth, 88(S02). A887-A906. https://doi.org/10.1029/JB088iS02p0A887

Matysiak, A. K. & Trepmann, C. A. 2015. The deformation record of olivine in mylonitic peridotites from the Finero Complex, Ivrea Zone: Separate deformation cycles

during exhumation. Tectonics, 34(12). 2514-2533. https://doi.org/10.1002/2015tc003904
Maulana, A., Christy, A. G. & Ellis, D. J. 2015. Petrology, geochemistry and tectonic significance of serpentinized ultramafic rocks from the South Arm of Sulawesi, Indonesia. Geochemistry, 75(1). 73-87. https://doi.org/10.1016/j.chemer.2014.09.003
Monnier, C., Girardeau, J., Maury, R. C. & Cotten, J. 1995. Back-arc basin origin for the East Sulawesi ophiolite (eastern Indonesia). Geology, 23(9). 851-854. https://doi.org/10.1130/0091-7613(1995)023<0851:Baboft>2.3.Co;2
Olfindo, V. S. V., Payot, B. D., Valera, G. T. V. & Arai, S. 2020. Petrogenesis of heterogeneous mantle peridotites with Ni-rich olivine from the Pujada Ophiolite, Philippines. Journal of Asian Earth Sciences: X, 4. https://doi.org/10.1016/j.jaesx.2020.100039
Parkinson, C. 1998. Emplacement of the East Sulawesi Ophiolite: evidence from subophiolite metamorphic rocks. Journal of Asian Earth Sciences, 16(1). 13-28. https://doi.org/10.1016/s0743-9547(97)00039-1
Payot, B., Arai, S., Yoshikawa, M., Tamura, A., Okuno, M. & Rivera, D. 2018. Mantle Evolution from Ocean to Arc: The Record in Spinel Peridotite Xenoliths in Mt. Pinatubo, Philippines. Minerals, 8(11). https://doi.org/10.3390/min8110515
Pearce, J. A., Lippard, S. J. & Roberts, S. 1984. Characteristics and tectonic significance of supra-subduction zone ophiolites. Geological Society, London, Special Publications, 16(1). 77-94. https://doi.org/10.1144/gsl.Sp.1984.016.01.06
Pittarello, L., McKibbin, S., Yamaguchi, A., Ji, G., Schryvers, D., Debaille, V. & Claeys, P. 2019. Two generations of exsolution lamellae in pyroxene from Asuka 09545: Clues to the thermal evolution of silicates in mesosiderite. American Mineralogist, 104(11). 1663-1672. https://doi.org/10.2138/am-2019-7001
Poli, S. & Schmidt, M. W. 2002. Petrology of Subducted Slabs. Annual Review of Earth and Planetary Sciences, 30(1). 207-235. https://doi.org/10.1146/annurev.earth.30.091201.140550
Rajesh, H. M. 2006. Progressive or continual exsolution in pyroxenes: an indicator of polybaric igneous crystallization for the Perinthatta anorthositic gabbro, northern Kerala, southwestern India. Journal of Asian Earth Sciences, 26(5). 541-553. https://doi.org/10.1016/j.jseaes.2004.11.004
Ray, D., Banerjee, R., Iyer, S. D. & Mukhopadhyay, S. 2010. A New Report of erpentinites from Northern Central Indian Ridge (at 6°S)-An Implication for Hydrothermal Activity. Acta Geologica Sinica - English Edition, 82(6). 1213-1222. https://doi.org/10.1111/j.17556724.2008.tb00723.x
Simandjuntak, T. O., Surono & Sukido 1993. Peta Geologi Lembar Kolaka, Sulawesi, Bandung, Pusat Penelitian dan Pengembangan Geologi.p.
Streckeisen, A. 1976. To each plutonic rock its proper name. Earth-Science Reviews, 12(1). 1-33. https://doi.org/10.1016/0012-8252(76)90052-0
Surono 2013. Geologi Lengan Tenggara Sulawesi, Bandung, Badan Geologi. 201 p.
Surono & Hartono, U. 2013. Geologi Sulawesi, Jakarta, LIPI Press. 352 p.
Syahrul. 2017. Studi Paragenesis dan Mineralisasi kompleks Batuan Ultramafik daerah Sopura, Kabupaten Kolaka, Provinsi Sulawesi Tenggara. Theses, Institut Teknologi Bandung.
van Zuidam, R. A. 1986. Aerial photo-interpretation in terrain analysis and geomorphologic mapping, Netherland, Publisher The Hague.p.
Whitney, D. L. & Evans, B. W. 2009. Abbreviations for names of rock-forming minerals. American Mineralogist, 95(1). 185-187. https://doi.org/10.2138/am.2010.3371
Yellappa, T., Koizumi, T. & Tsunogae, T. 2021. Geochemical constrains on pyroxenites from Aniyapuram Mafic–Ultramafic Complex, Cauvery Suture Zone, southern India: Suprasubduction zone origin. Journal of Earth System Science, 130(1). https://doi.org/10.1007/s12040-020-01516-8
Zeng, Z., Wang, Q., Wang, X., Chen, S., Yin, X. & Li, Z. 2012. Geochemistry of abyssal peridotites from the super slow-spreading Southwest Indian Ridge near 65°E: Implications for magma source and seawater alteration. Journal of Earth System Science, 121(5). 1317-1336. https://doi.org/10.1007/s12040-012-0229-z